

Problem-dependent attention and effort in neural networks with an application to image resolution

Chris Rohlf^{1,2*}

^{1*}Wealth Management Strats & Modeling, Morgan Stanley, 1221 Avenue of the Americas Fl 5, New York, 10020, New York, USA.

²Department of Electrical Engineering, Columbia University, 500 West 120th Street, Fl 13, New York, 10027, New York, USA.

Corresponding author(s). E-mail(s): car2228@columbia.edu;

Abstract

This paper introduces a new neural network-based estimation approach that is inspired by the biological phenomenon whereby humans and animals vary the levels of attention and effort that they dedicate to a problem depending upon its difficulty. The proposed approach leverages alternate models' internal levels of confidence in their own projections. If the least costly model is confident in its classification, then that is the classification used; if not, the model with the next lowest cost of implementation is run, and so on. This use of successively more complex models—together with the models' internal propensity scores to evaluate their likelihood of being correct—makes it possible to substantially reduce resource use while maintaining high standards for classification accuracy. The approach is applied to the digit recognition problem from Google's Street View House Numbers dataset, using Multilayer Perceptron (MLP) neural networks trained on high- and low-resolution versions of the digit images. The algorithm examines the low-resolution images first, only moving to higher resolution images if the classification from the initial low-resolution pass does not have a high degree of confidence. For the MLPs considered here, this sequential approach enables a reduction in resource usage of more than 50% without any sacrifice in classification accuracy.

Keywords: downsampling, attention, effort, deep learning, machine learning

1 Introduction

Any model of optimal research activity will generate the prediction that the effort expended increases with the importance and difficulty of the problem. Optimizing behavior of this form is ubiquitous in humans and other animals. The cost of in-depth analysis should only be incurred for problems that cannot be solved through simpler means. In biological systems, the selection of cases for learning is typically curiosity-driven, with new observations selected because they have some new features not captured by the existing framework (Sinz *et al.* 2019 [1]). By contrast, many artificial neural networks—and machine learning systems more generally—apply a standardized and uniform process to all observations without regard to the information value of different training cases or the difficulty or confidence of classifying different test cases. Artificial neural networks are known to be considerably more demanding of resources than their biological counterparts (*cf.* Perry, Barron, and Chittka 2017 [2], Scheffer *et al.* 2020 [3]), and there is potential to generate considerable value through improving the judiciousness with which artificial systems consume data and computational resources.

The current study introduces and applies a new conceptual framework for making tradeoffs between the difficulty of classifying a given test case and the complexity of the model and data that are applied. In the approach described in section 2, multiple trained models with varying degrees of complexity and resource intensity are at the researcher’s disposal. When faced with a new test case, the simplest and least resource-intensive model is applied first. If the simple approach produces a classification with a high degree of confidence (above some specified threshold), then that classification is used. Otherwise, the process is repeated with the next higher level of model and data complexity. This sequential process conserves resources by classifying the relatively straightforward test cases quickly without resorting to the use of more complex approaches. It nevertheless preserves the accuracy of the forecasts by only using the results of the simpler approaches when the confidence in those projections is high.

To determine whether the simpler approach’s forecast is used, the model’s internal propensity score for the chosen classification is used as its level of confidence in its projection. In a digit classification application, for example, if the model assigns equal likelihood to a test image being a one or a seven, then the propensity score is relatively low (50% or less); thus, a closer examination with a more complex model may be warranted. But if the model projects a classification of three with 95% likelihood, then it is likely that further analysis would not be worth the cost.

This multi-stage strategy of problem-dependent effort is applied to a digit classification exercise using Google’s well-known Street View House Numbers (SVHN) dataset [4]. Each input image in the dataset is 32 x 32 pixels of red blue and green, constituting 3,072 bytes of data. For each image, downsampled low-resolution versions with sizes of 16 x 16, 8 x 8, and 4 x 4 pixels. Separate Multilayer Perceptron (MLP) neural networks are trained on the full datasets

of each of the four image resolutions. For each test case, analysis is first performed on the low-resolution thumbnail image. Successively higher resolution images (and the trained MLPs corresponding to those resolution levels) are only applied in those cases when the prior models lack confidence in their projections. For the MLPs estimated here on the SVHN data, the results indicate that data usage could be reduced by more than 50% without any compromise in performance and that slight improvements in performance are possible relative to the benchmark model that only examines the high-resolution images. The results also map out the rates at which classification accuracy can be sacrificed to achieve even more substantial savings in data usage.

The application presented here is intended as a proof of concept to illustrate the potential for the use of problem-dependent effort in classification. The SVHN dataset and its components are not large, nor are the resource demands of the most complex classifier examined here. Nevertheless, the question of excessive resource use in artificial neural networks is an important one, and the tools presented and demonstrated in this study provide an intuitive and easy-to-use way to achieve substantial reductions in model complexity while maintaining high standards of forecasting accuracy. In some practical cases of network-based classification, critical tradeoffs must be made between the costs and benefits of high resolution images, as with the chest x-ray data examined by Sabottke and Spieler (2020) [5]. As the demand for speed, scalability, and performance for neural networks continues to grow, so will the value of thoughtful ways to address such tradeoffs. Many researchers have found that classification exercises depend more crucially upon broad patterns in the data—such as the local averages of Convolutional Neural Networks or correlations in pixel intensities across color channels, as in Holistic Attention Networks (Lecun *et al.* 1998 [6], Niu *et al.* 2020 [7])—that do not necessarily require the high level of granularity of the original data. Wang *et al.* (2020) [8] also find that using copies of an image with different resolutions can help neural networks to identify such patterns. Image resolution is known to have noticeable impacts on neural networks’ classification performance (Koziarski and Cyganek 2018 [9]). Resolution does pose less of a constraint than it once did, however, and researchers now use neural network-based “super-resolution” approaches to identify what higher resolution images could be expected to look like based upon lower resolution data (*cf.* Yang *et al.* 2019 [10]).

A key contribution of the current study is to highlight the value of machine learning and deep learning models’ propensity scores as underutilized measures of classification accuracy. The analysis in section 4 of this study shows that the propensity scores produced by the MLPs estimated here provide reliable proxies for the performance of the models on test cases. While the application in this study uses Multilayer Perceptron (MLP) neural network-based classifiers, any classification approach could in principle be used, provided that it projects continuous likelihoods of each of the possible categories for each test case. Moreover, the use of propensity scores need not be limited to the sequential problem-dependent effort framework presented here. Even when data usage

and model complexity are not especially costly, multiple classifiers' propensity scores could be compared so that the classifier with the highest level of confidence is always used—producing a multi-model classifier with greater accuracy than any of its constituents in a manner analogous to boosting (*cf.* Schapire and Freund 2012 [11]).

2 Conceptual Framework

Figure 1 illustrates the original and downsampled representations of images that are the focus of this study. Panel 1a presents visually the first test observation from the well-known SVHN dataset, using the “cropped digits” variant. Each pixel's color is determined by three bytes of data giving the intensities of the red, green, and blue hue. Hence, an uncompressed representation of the 32 x 32 image takes up $32 * 32 * 3 = 3,072$ bytes of storage or bandwidth. The classifier employed in this analysis consumes these 3,072 one-byte pixel intensities (numbers from 0 to 255) as inputs and returns a value from 0 to 9 giving the model's projection of what digit is represented in the image. Panels 1b, 1c, and 1d present 16 x 16, 8 x 8, and 4 x 4 pixel representations of the same image, where the images are shrunk using bicubic interpolation (the `imresize` function in Matlab). These downsampled 16 x 16, 8 x 8, and 4 x 4 images in turn take up 768, 192, and 48 bytes, respectively. As this example illustrates, the 32 x 32 and 16 x 16 representations in the first two panels are straightforward for a human to correctly classify as the number 5 with a high degree of confidence, but the problem becomes more difficult as the amount of downsampling increases.

When performing large-scale or time-critical classification tasks, it may be desirable to sacrifice some degree of accuracy in order to reduce the amount of data required for the classification task. The engineering problem considered here is to perform this tradeoff between accuracy and data usage in a case-specific way, so that for easier tasks, the thumbnail versions of the images can be used, but if the neural network has a low level of confidence in its projected classification, then the more granular representation of the image is pulled and analyzed.

This sequential process—in which coarse data are analyzed first and granular data may or may not be used—is diagrammed in the flow chart in Figure 2, which presents the steps performed to classify a single test case in the SVHN dataset. The research has access to an array of trained models with varying degrees of complexity and resource intensity, each of which can be applied to a given test case. Step 1 initializes the iteration number at $t = 0$, when the coarsest representation of the image (the 4 x 4 representation as shown in panel 1d) is extracted in step 2. A neural network is then used in step 3 to assign probabilities $p_0...p_9$ to each of the possible classifications. For the purposes of this analysis, let these model-specific probabilities be denoted propensities. Next, step 4 determines how confident the model is in its classification examining the distribution of these propensities across the 10 categories. If the propensities are concentrated on one classification—in the extreme case 100% for one

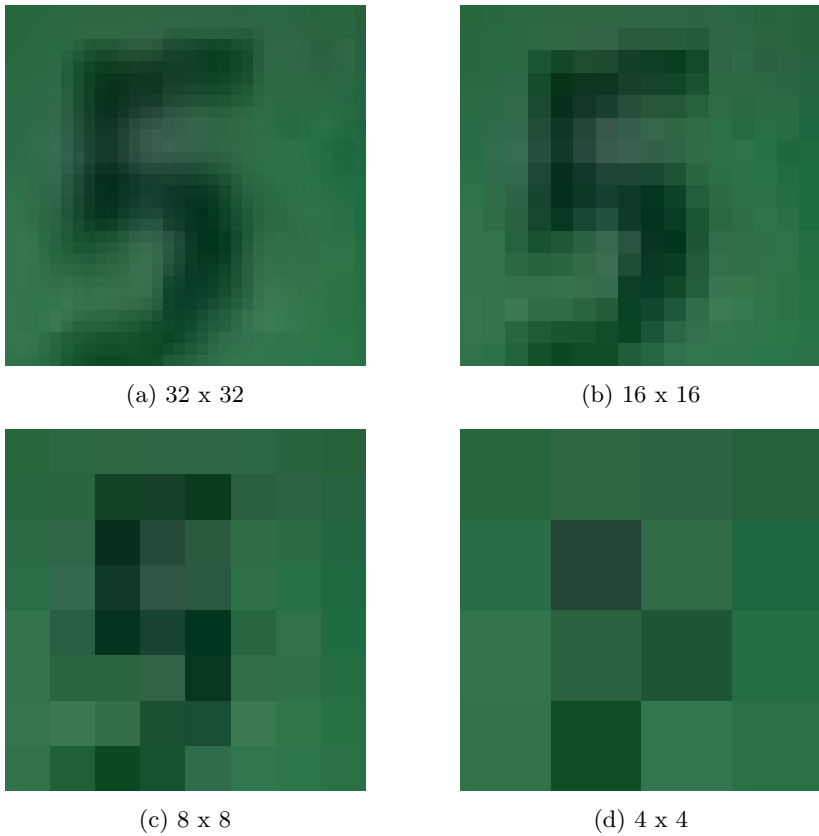


Fig. 1: Example SVHN image at different resolution levels

category and 0% for the others—then the classifier is highly confident in its selection. If the propensities are relatively spread out—in the extreme case with values of 10% for each of the 10 categories—then the model and data provide little information value, and the classifier has little confidence in its selection. Step 4 compares the propensity score for the most promising candidate classification to some threshold propensity level. If the classifier is highly confident in its selection, then the classifier stops at stage 5 and chooses this category with the highest propensity score. If the classifier’s level of confidence in its choice falls below the threshold, then the iterator t increments by one, and the process repeats with a slightly larger image—in this case, the 8 x 8 representation as in panel 1c.

3 Estimation Approach

The data used in this analysis are the “cropped digit” images from Google’s Street View House Numbers (SVHN) dataset [4]. This well-known dataset

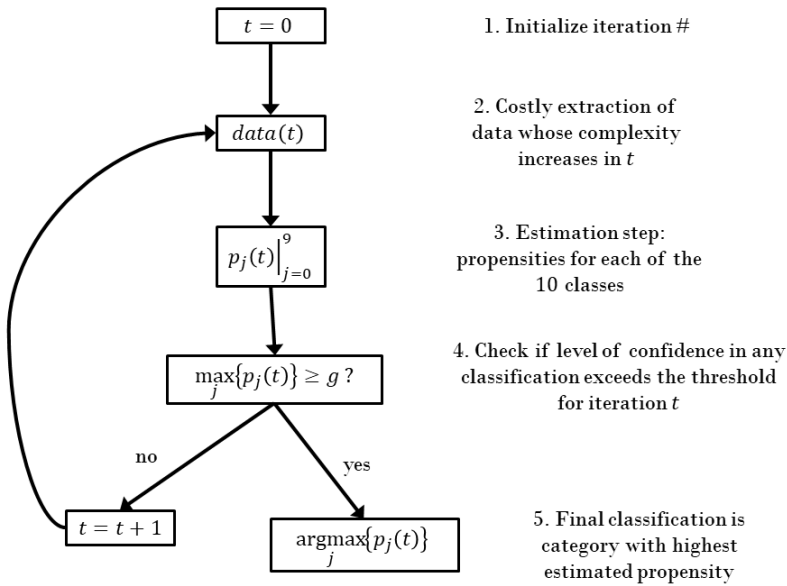


Fig. 2: Flow Chart Illustrating Deployment of Problem-Dependent Effort Classifier on a Single Test Case

contains 73,257 images that are designated to be used for training and 26,032 to be used for testing. For the current setting, the training data is split further, with the last 10% of cases (7,325 images) used for validation and the remaining 65,932 used for training. The numbers of cases are not equal across digit types, with disproportionately more ones and twos (19.1% and 14.8%) and fewer nines and zeros (6.3% and 6.7%). The respective images' raw pixel intensities are used without normalization.

Four fully-connected multilayer perceptron (MLP) neural networks are estimated using the training and validation sets, one for each image coarseness category. The vector of true digit labels is the same across all four sets of images, and each of these MLP networks is trained and validated to maximize the fraction of accurate classifications for these labels. The configurations of these MLP networks are described in Table 1. Each of these configurations was selected from a handful of candidate specifications based upon its classification accuracy for the validation set. The networks have varying degrees of breadth and depth that increase with the complexity of the input data. The number of hidden layers ranges from 30 for the 4×4 images to 46 for the 32×32 images, and the number of hidden nodes ranges from 5,800 to 62,400—so that the number of nodes per hidden layer varies from 193.3 for the smallest images to 1,356.5 for the largest images. Each of the MLP configurations follows a symmetric hourglass shape, with the largest hidden layers at the

beginning and end and the smallest hidden layers in the middle. Each hidden layer appears in sequence, so that the MLP for the 4 x 4 images contains a 48-node input layer, a 300-node hidden layer, a second 300-node hidden layer, a sequence of ten 200-node hidden layers, and so on, ending with a sequence of two 300-node hidden layers followed by a 10-node output layer.

Image size	32x32	16x16	8x8	4x4
Layer type	Nodes			
Input layer	3,072	768	192	48
Hidden layers		2 of 4,800		
		2 of 2,400		
	3 of 4,800	2 of 1,200	2 of 2,400	
	3 of 2,400	4 of 600	2 of 1,200	
	3 of 1,200	2 of 300	2 of 600	2 of 300
	6 of 600	2 of 200	6 of 400	10 of 200
	16 of 300	4 of 150	11 of 200	6 of 100
	6 of 600	2 of 200	6 of 400	10 of 200
	3 of 1,200	2 of 300	2 of 600	2 of 300
	3 of 2,400	4 of 600	2 of 1,200	
	3 of 4,800	2 of 1,200	2 of 2,400	
		2 of 2,400		
		2 of 4,800		
Output layer	10	10	10	10
Total hidden layers	46	32	35	30
Total hidden nodes	62,400	41,000	23,800	5,800

Table 1: Node and layer configurations for four multilayer perceptrons

Each of the nodes uses a hyperbolic activation function, and the final output layer is a logistic regression. The weights for each of the connections, including the coefficients in the logistic regression layer, are estimated via gradient descent with a learning rate of 0.01 and batch size of 200. Estimation is performed on a GPU using the **theano** package in Python following the general structure provided by the Theano Development Team (2013) [12] but with modifications so that, for the iteration in which the optimum is achieved, the propensity scores and chosen classifications for the are output for each training, validation, and test case.

In principle, any type of classifier could be used, and the classifier type could vary across the different input image sizes. An MLP is used rather than a Convolutional Neural Network (CNN) for consistency and transparency. Because the impact of image resolution is a key focus for this analysis, the local averaging of CNNs is not used so that specific pixels' intensity values enter into the neural network directly as inputs. Additionally, local averaging such as that used by CNNs is not well-suited to the already shrunken 4 x 4 images, and using the same style of network facilitates comparisons across the different networks.

In the hypothetical bandwidth- or storage-saving scenario that represents the intended use of the approach, the parameter values for all four MLPs would first be determined from the training and validation data. Then, at

the deployment stage for a given test case, the smallest thumbnail image is downloaded and processed first, and larger images are only used if the MLP for the smaller image has a low level of confidence in its forecast. For the current study, which demonstrates the application and effectiveness of the proposed multi-stage MLP approach described in Figure 2, all four MLPs are applied to every test case, so that all four MLPs' classifications and propensity scores are available for comparison. Given this full set of propensity scores and classifications, the analysis in section 4 examines the levels of accuracy and data-savings that can be achieved at different thresholds g .

4 Empirical Results

Table 2 presents the performance of the four MLP classifiers described in Table 1 on each of the training, validation, and test samples from the SVHN data. The fraction of digits that are correctly classified is shown, where pure random selection would produce accuracy rates of 10%. As the table shows, given the selected MLP configurations, the ability to correctly classify training, validation, and test cases increases substantially with the amount of input data used. For the 4 x 4 images, the MLP with 30 hidden layers and 5,800 hidden nodes accurately classifies 40.2% of the test cases and exhibits similar performance on the training and validation sets. Roughly twice as many test cases are correctly classified when the 32 x 32 images are used together with the MLP that has 46 hidden layers and 62,400 hidden nodes. The classifiers that use more complex data and neural networks exhibit more overfitting, so that advantage for the larger images and more complex networks is even greater for training cases than for test cases. As the images become larger, the amount of data required to represent each case increases geometrically, and the incremental improvement in classification accuracy declines. The 16 x 16 MLP accurately classifies 79.1% of test cases, nearly as many as the 32 x 32 MLP. This closeness in the rates of correct classification between the two types of input images demonstrates that the amount of data usage can be substantially reduced without large declines in performance.

Image Size	32x32	16x16	8x8	4x4
Sample	% Correctly Classified			
Training (N=65,932)	87.9%	85.6%	66.3%	40.8%
Validation (N=7,325)	82.5%	81.7%	65.2%	40.5%
Test (N=26,032)	80.7%	79.1%	65.5%	40.2%

Table 2: Performance of multilayer perceptron classifiers on SVHN samples

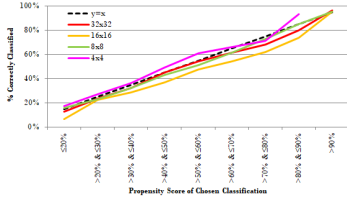
Returning to the visual representations of the first test case presented in Figure 1, the MLP for 4 x 4 images correctly classified that case as a 5, but its propensity score was 34.4%, indicating that it did not have a high degree of confidence in that classification. The MLP for the 8 x 8 images incorrectly classified the image in panel 1c as a 6 and had fairly high degree of confidence

of 74.3% in that classification. the MLPs for the 16 x 16 and 32 x 32 images both correctly classified the image as a 5. The 16 x 16 classifier was highly confident in its categorization, assigning a propensity score of 97.4%, while the 32 x 32 classifier was less so, giving a propensity score of 54.5%.

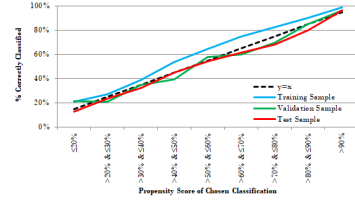
A key requirement for the effective implementation of the approach described in section 2 is that the MLPs' case-specific propensity scores are informative about the likely accuracy of the model's classification for those cases. The point is addressed in Figure 3, which presents the fraction of cases that are correctly classified as it varies with the MLP-specific propensity scores for those cases. Panel 3a plots these relationships for the test samples for each of the four size-specific MLPs. The horizontal axis plots nine different propensity score ranges from $\leq 20\%$, 20% to 30%, and so on up to $> 90\%$. Because the ten propensities add to 100%, the maximum propensity score is guaranteed to be at least 10% for each case. The vertical axis plots the fraction of test cases that are correctly classified by the models among those cases whose model-specific propensities fall into the relevant propensity score ranges. The dashed black line is 45 degrees from the horizontal axis, with values of 15%, 25%, . . . , up through 95%. Supposing that the propensity scores are uniformly distributed within each of the nine bins, this line plots the fraction correctly classified that would be observed if the propensity scores were exact measures of accuracy. The red, orange, green, and magenta lines in panel 3a show the fractions of test cases correctly classified within each bin for each of the image size and MLP combinations. The blue, green, and red lines in panel 3b show the fractions correctly classified within each bin for the MLP for the 32 x 32 images on each of the training, validation, and test samples.

For the approach outlined in this study to work, the red, orange, green, and magenta lines in panel 3a do not need to exactly align with the dashed black line. What is important is that there is a positive slope, so that the propensity scores are informative. That condition is satisfied, and the relationship is monotone increasing for all four samples. The lines are generally close to the dashed 45-degree line, though with some variation across the MLPs—with the 16 x 16 classifier generally underperforming its propensity scores slightly and the 4 x 4 classifier slightly overperforming its propensity scores. As the lines in panel 3b show, the relationship between propensity scores and correct classification by the 32 x 32 MLP is similar between the validation and test samples. The rates of correct classification in the training sample consistently exceed the 45-degree line, consistent with the pattern of overfitting in the training sample that was seen in Table 2.

Given that the propensity scores are predictive of test performance, Figure 4 illustrates the variation in these scores across MLPs and samples. The layout is the same as in Figure 3 but with the proportion of the sample plotted on the vertical axis, so that the graphs represent histograms. The evidence from panel 4a illustrates some of the same patterns shown in Table 2 and panel 3a but with some additional detail. Given that the rates of accuracy vary across the size-specific MLPs—and given that propensity scores are effective proxies



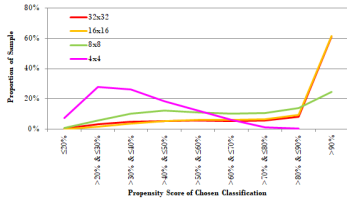
(a) By image size for the test sample



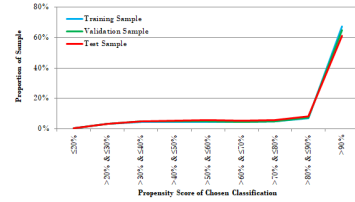
(b) By sample for full-sized images

Fig. 3: Fraction of cases correctly classified by propensity scores

for accuracy—the propensity scores are expected to vary across the MLPs in the manner shown, with greater concentration among lower propensity scores for the 4 x 4 images and greater concentrations of high propensity scores for the 32 x 32 and 16 x 16 images. For the 4 x 4 images, roughly half of the data falls into the 20% to 40% propensity score ranges, and no cases appear in the highest > 90% category. For the 8 x 8 images, the propensity scores are more evenly distributed, with more than 20% of the sample in the highest category. The propensity score distributions are similar for the 16 x 16 and 32 x 32 categories, with roughly 60% of the test sample in the > 90% category for both image sizes. As panel 4b shows, for the full-sized images, the distributions of propensity scores are similar between the training, validation, and test samples.



(a) By image size for the test sample



(b) By sample for full-sized images

Fig. 4: Fractions of cases with different propensity scores

Next, using the projected test sample classifications and propensity scores for the four MLP models, Table 3 applies the threshold-based multi-stage classification procedure laid out in Figure 2. Column (1) shows the results of the benchmark approach of exclusively using the MLP for the 32 x 32 images, with no downsampling. Column (2) shows the results of examining all four MLPs' classifications and choosing the one with the highest propensity score for each test case. Columns (3) to (8) then show the results of using threshold rules with different values for g , ranging from 90% down to 40%. The first row of percentages shows the top-line result: the fraction of test cases correctly classified when that procedure is used. The second row shows the average propensity score associated with the classification that is used. The next three

rows indicate the proportions of test cases for which the costly data extract was incurred for the 32 x 32, 16 x 16, 8 x 8, and 4 x 4 images. The last row shows the number of bytes read, which is obtained by multiplying these usage fractions by 3,072 for the 32 x 32 image, 768 for the 16 x 16 image, 192 for the 8 x 8 image, and 48 for the 4 x 4 image.

As the results from the table illustrate, there is considerable potential through the proposed approach to reduce data usage while maintaining a high level of classification accuracy. The benchmark approach presented in column (1) correctly classifies 80.7% while reading 3,072 bytes per case. When a 90% propensity score threshold is used in column (3), however, the proportion of test cases that are correctly classified is almost exactly the same at 80.8%, but the data usage is more than a third lower at 1,921 bytes per case. Much of this savings is obtained by relying upon the 16 x 16 images, for which the classifier’s accuracy is very close to that of the 32 x 32 MLP. Even for this 90% threshold classifier, however, it is possible to classify roughly a fourth of the test cases based upon the 8 x 8 image.

	(1)	(2)	(3)	(4)	(5)	(6)	(7)	(8)
	Benchmark	Best of 4	90%	Propensity Threshold 80%	70%	60%	50%	40%
% Correctly Classified	80.7%	80.9%	80.8%	80.1%	78.6%	75.6%	70.3%	62.6%
Average Propensity Score	83.0%	90.2%	84.7%	84.6%	83.3%	79.9%	73.5%	64.1%
% Used 32x32 Image	100.0%	100.0%	35.9%	25.1%	17.9%	11.4%	5.71%	1.75%
% Used 16x16 Image	0.0%	100.0%	75.4%	61.4%	50.4%	38.5%	25.2%	12.1%
% Used 8x8 Image	0.0%	100.0%	100.0%	99.8%	98.5%	92.4%	80.2%	61.7%
% Used 4x4 Image	0.0%	100.0%	100.0%	100.0%	100.0%	100.0%	100.0%	100.0%
Average Bytes Read	3,072	4,080	1,921	1,483	1,175	871.6	571.1	313.2

Table 3: Correctness, average propensity score, and data usage for different multi-stage MLPs

To better illustrate the tradeoffs between classifier accuracy and data usage, Figure 5 plots % Correctly Classified against Average Bytes Read for all possible thresholds from 10% to 100%. The magenta line illustrates these combinations for the threshold-based classifier whose results are presented in Table 3, where the image size at $t = 0$ is 4 x 4. As the usage percentages in that table show, the 4 x 4 MLP’s classification is rarely used for moderate to high propensity score thresholds. For this reason, two alternative multi-stage threshold-based MLP classifiers are considered in Figure 5. The green line shows the possible combinations of accuracy and data usage when the image size at $t = 0$ is 8 x 8—which eliminates the initial 48-byte expenditure on reading the 4 x 4 image and starts the classifier at the higher baseline accuracy rate of the 65.5% achieved by the 8 x 8 MLP classifier. Similarly, the orange line shows the possible combinations of accuracy and data usage when the image size at $t = 0$ is 16 x 16. As all three lines show, it is possible to maintain high standards of classification accuracy while considerably reducing data usage relative to the 3,072 bytes required by the benchmark classifier. Some notably strong performance arises from the classifier that begins with

the 16 x 16 image. For threshold values between 62% and 67%, this threshold-based multi-stage MLP correctly classifies 80.7% of cases—the same rate as is achieved by the benchmark—with data consumption of only 1,319 to 1,409 bytes, 42.9% to 45.9% of the 3,072 bytes required in the benchmark case. At threshold values of 83% to 88%, the classifier beginning with the 16 x 16 images achieves its peak accuracy rate of 81.1%, with data consumption ranging from 1,732 bytes to 1,873 bytes.

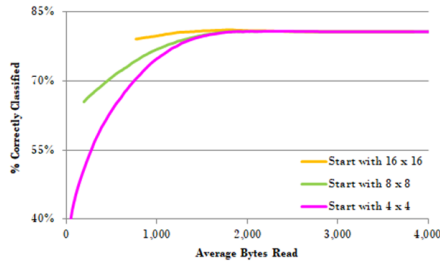


Fig. 5: Possible combinations of classification accuracy and data usage using different multi-stage MLP classifiers

5 Conclusion

This study presents a new framework for reducing the resource intensity of AI-based classification approaches while maintaining high standards for accuracy. The strategy is inspired by biological approaches to attention and information-gathering whereby the amount of effort expended increases with the difficulty of the problem. Analysis begins with a simplified classification model applied to a parsimonious representation of the data. A threshold-based approach is used based upon the model’s internal level of confidence in its classification. If the simple model has a high degree of confidence in its classification, then that label is used. If, however, the coarse version of the data is not sufficiently informative to produce a classification with a high degree of confidence, then a more granular representation of the test case is analyzed.

The approach is applied to Google’s Street View Housing Numbers (SVHN) dataset, with digit classification performed using Multilayer Perceptron (MLP) networks. Low-resolution versions of the images are analyzed first to produce initial classifications, and higher-resolution versions are only analyzed for cases in which the model does not have a high degree of confidence in its initial classification. When compared with a benchmark MLP classifier that only uses the high-resolution data, the threshold-based classifier can achieve the same level of accuracy with less than half the data usage. Further reductions in data usage can be achieved with relatively little sacrifice in performance. Additionally, in some cases, the threshold-based MLP approach is found to

slightly improve classification accuracy at the same time as it reduces data intensity.

References

- [1] Sinz, F.H., Pitkow, X., Reimer, J., Bethge, M., Tolias, A.S.: Engineering a less artificial intelligence. *Neuron* **103**, 967–79 (2019)
- [2] Perry, C.J., Barron, A.B., Chittka, L.: The frontiers of insect cognition. *Current Opinion in Behavioral Sciences* **16**, 111–8 (2017)
- [3] Scheffer, L.K., Xu, C.S., Januszewski, M., Lu, Z., Takemura, S., Hayworth, K.J., Huang, G.B., Shinomiya, K., Maitlin-Shepard, J., Berg, S., Clements, J., Hubbard, P.M., Katz, W.T., Umayam, L., Zhao, T., Ackerman, D., Blakely, T., Bogovic, J., Dolafi, T., Kainmueller, D., Kawase, T., Khairy, K.A., Leavitt, L., Li, P.H., Lindsey, L., Neubarth, N., Olbris, D.J., Otsuna, H., Trautman, E.T., Ito, M., Bates, A.S., Goldammer, J., Wolff, T., Svirskas, R., Schlegel, P., Neace, E., Knecht, C.J., Alvarado, C.X., Bailey, D.A., Ballinger, S., Borycz, J.A., Canino, B.S., Cheatham, N., Cook, M., Dreher, M., Duclos, O., Eubanks, B., Fairbanks, K., Finley, S., Forknall, N., Francis, A., Hopkins, G.P., Joyce, E.M., Kim, S., Kirk, N.A., Kovalyak, J., Lauchie, S.A., Lohff, A., Maldonado, C., Manley, E.A., McLin, S., Mooney, C., Ndama, M., Ogundeyi, O., Okeoma, N., Ordish, C., Padilla, N., Patrick, C.M., Paterson, T., Phillips, E.E., Phillips, E.M., Rampally, N., Ribeiro, C., Robertson, M.K., Rymer, J.T., Ryan, S.M., Sammons, M., Scott, A.K., Scott, A.L., Shinomiya, A., Smith, C., Smith, K., Smith, N.L., Sobeski, M.A., Suleiman, A., Swift, J., Takemura, S., Talebi, I., Tarnogorska, D., Tenshaw, E., Tokhi, T., Walsh, J.J., Yang, T., Horne, J.A., Li, F., Parekh, R., Rivlin, P.K., Jayaraman, V., Costa, M., Jefferis, G.S.X.E., Ito, K., Saalfeld, S., George, R., Meinertzhagen, I.A., Rubin, G.M., Hess, H.F., Jain, V., Plaza, S.M.: A connectome and analysis of the adult *drosophila* central brain. *eLife* **9** (2020)
- [4] Netzer, Y., Wang, T., Coates, A., Bissacco, A., Wu, B., Ng, A.Y.: Reading digits in natural images with unsupervised feature learning. *NIPS Workshop on Deep Learning and Unsupervised Feature Learning* <http://ufldl.stanford.edu/housenumbers> (2011)
- [5] Sabottke, C.F., Spieler, B.M.: The effect of image resolution on deep learning in radiography. *Radiology: Artificial Intelligence* **2** (2020)
- [6] LeCun, Y., Bottou, L., Bengio, Y., Haffner, P.: Gradient-based learning applied to document recognition. *Proceedings of the IEEE* **86**, 2278–324 (1998)
- [7] Niu, B., Wen, E., Ren, W., Zhang, X., Yang, L., Wang, S., Zhang, K., Cao, X., Shen, H.: Single image super-resolution via a holistic attention

- network. European Conference on Computer Vision (ECCV), 191–207 (2020)
- [8] Wang, F., Eljarrat, A., Muller, J., Hennien, T.R., Erni, R., Koch, C.T.: Multi-resolution convolutional neural networks for inverse problems. *Scientific Reports* **10** (2020)
 - [9] Koziarski, M., Cyganek, B.: Impact of low resolution with deep neural networks: an experimental study. *International Journal of Applied Mathematics and Computer Science* **28**, 735–44 (2018)
 - [10] Yang, W., Zhang, X., Tian, Y., Wang, W., Xue, J., Liao, Q.: Deep learning for single image super-resolution: a brief review. *IEEE Transactions on Multimedia* **21**, 3106–21 (2019)
 - [11] Schapire, R.E., Freund, Y.: *Boosting: Foundations and Algorithms*. MIT Press, Cambridge, MA (2012)
 - [12] Theano Development Team: Multilayer Perceptron. <https://deeplearning.net/tutorial/mlp.html> (2013)